Taylor & Francis
Taylor & Francis Group

BASIC RESEARCH PAPER

Metabolic effects of fasting on human and mouse blood in vivo

Federico Pietrocola[a,b,c,d,†], Yohann Demont[a,b,c,†], Francesca Castoldi[a,b,c,d,f,†], David Enot[a,d], Sylvère Durand[a,d], Michaela Semeraro[a,e], Elisa Elena Baracco[a,b,c,d], Jonathan Pol[a,b,c,d], Jose Manuel Bravo-San Pedro[a,b,c,d], Chloé Bordenave[a,d], Sarah Levesque[a,b,c,d], Juliette Humeau[a,b,c,d], Alexis Chery[a,d], Didier Métivier[a,b,c], Frank Madeo[g,h], M. Chiara Maiuri[a,b,c,d,#], and Guido Kroemer[a,b,c,d,i,j,#]

aEquipe 11 labellisée Ligue contre le Cancer, Centre de Recherche des Cordeliers, INSERM U 1138, Paris, France; bUniversité Paris Descartes, Sorbonne Paris Cité, Paris, France; cUniversité Pierre et Marie Curie, Paris, France; dMetabolomics and Cell Biology Platforms, Gustave Roussy Comprehensive Cancer Institute, Villejuif, France; eCentre d'Investigation Clinique-Unité de Recherche Clinique Paris Centre Necker-Cochin, Assistance Publique Hôpitaux de Paris, France; fSotio a.c.; Prague, Czech Republic; gInstitute of Molecular Biosciences, NAWI Graz, University of Graz, Graz, Austria; hBioTechMed-Graz, Graz, Austria; iPôle de Biologie, Hôpital Européen Georges Pompidou, AP-HP, Paris, France; jKarolinska Institute, Department of Women's and Children's Health, Karolinska University Hospital, Stockholm, Sweden

ABSTRACT

Starvation is a strong physiological stimulus of macroautophagy/autophagy. In this study, we addressed the question as to whether it would be possible to measure autophagy in blood cells after nutrient deprivation. Fasting of mice for 48 h (which causes ~20% weight loss) or starvation of human volunteers for up to 4 d (which causes <2% weight loss) provokes major changes in the plasma metabolome, yet induces only relatively minor alterations in the intracellular metabolome of circulating leukocytes. White blood cells from mice and human volunteers responded to fasting with a marked reduction in protein lysine acetylation, affecting both nuclear and cytoplasmic compartments. In circulating leukocytes from mice that underwent 48-h fasting, an increase in LC3B lipidation (as assessed by immunoblotting and immunofluorescence) only became detectable if the protease inhibitor leupeptin was injected 2 h before drawing blood. Consistently, measurement of an enhanced autophagic flux was only possible if white blood cells from starved human volunteers were cultured in the presence or absence of leupeptin. Whereas all murine leukocyte subpopulations significantly increased the number of LC3B+ puncta per cell in response to nutrient deprivation, only neutrophils from starved volunteers showed signs of activated autophagy (as determined by a combination of multi-color immunofluorescence, cytofluorometry and image analysis). Altogether, these results suggest that white blood cells are suitable for monitoring autophagic flux. In addition, we propose that the evaluation of protein acetylation in circulating leukocytes can be adopted as a biochemical marker of organismal energetic status.

Introduction

Autophagy, a lysosomal bulk degradation process that allows cells to adapt to stress, to mobilize their energetic reserves, and to degrade potentially harmful constituents, is one of the cardinal determinants of cellular and organismal homeostasis in conditions of starvation, infection, cardiovascular disease or neoplasia.[1-5] Nutritional, behavioral, pharmaceutical or genetic manipulations designed to increase longevity in model organisms uniformly induce autophagy (whenever autophagy has been measured), suggesting that an increase in autophagic flux may constitute an obligate step for improving health span and life span.[6-10] Indeed, in all cases in which autophagy has been inhibited by suitable genetic interventions, the beneficial effects of anti-aging and life-span-extending manipulations has been negated, supporting a role for autophagy in determining the frontier between health and disease.[11-13]

In view of the major role of autophagy in the pathophysiology of disease,[14] there is a widespread quest for an ideal way to measure autopagic flux[15,16] by means of a hypothetical assay that would constitute the ideal "autophagometer."[17,18] Driven by this consideration, we sought to determine whether it would be possible to measure autophagy in a minimally invasive fashion in circulating white blood cells from mice or healthy human volunteers exposed to the most physiological stimulus of autophagy, which is nutrient deprivation. Starvation from macronutrients induces autophagy in a highly efficient fashion, in vitro and in vivo.[19] Starvation leads to a global decrease in protein acetylation in cells due to the combined increase in the enzymatic activity of protein deacetylases (in particular

sirtuins) and the decrease in the activity of acetyltransferases (in particular EP300 [E1A binding protein p300]).[20-23]

Based on these premises, we decided to measure protein acetylation and autophagy in leukocytes from mice or healthy persons in conditions of obligatory or voluntary starvation, respectively. Here, we report that we were able to measure protein deacetylation in leukocytes from starved mice and healthy volunteers that agreed to start a period of up to 5 d of fasting. In these settings, we could also detect signs of enhanced autophagy both in murine white blood cells and in cultured leukocytes derived from fasted individuals. Although preliminary, these results reveal the possibility to conceive, either directly (for animal experiments) or indirectly (for humans), a noninvasive 'autophagometer' to evaluate autophagic flux at the organismal level.

Results

Alterations in the metabolome induced by starvation

Starvation of humans for several (2–4) d caused a dramatic increase in multiple distinct free fatty acids, acylcarnitine species and the oxidized amino acid dimer cystine, as well as a significant decrease in tryptophan, choline phosphate, hippuric acid and glycerophosphocholine in plasma (Fig. 1A, Fig. S1, Table S1). In contrast, the alterations in the intracellular metabolome of circulating leukocytes were much less pronounced, with an increase in hydroxybutyrylcarnitine as the sole

significant increase (Fig. 1B, Fig. S1, Table S1). Hence, it appears that the intracellular compartment (represented by leukocytes) is much less affected by nutrient deprivation than the extracellular fluid (represented by plasma). Very similar results were obtained upon starvation of mice for a 48-h period. Again, the changes in the plasma metabolome were far more dramatic than those in the leukocyte metabolome. In mice, the plasma concentration of multiple acylcarnitine species (including hydroxybutyrylcarnitine), free fatty acids, and glucocorticoids tended to increase, while the concentrations of several amino acids (arginine, methionine, proline, etc.) significantly decreased (Fig. 2A, Fig. S1, Table S1). Again, the variations in the intracellular metabolome of circulating while blood cells were far less pronounced and barely significant (Fig. 2B, Fig. S1, Table S1). These results corroborate the idea that the intracellular metabolome is "buffered" by homeostatic mechanisms against variations in extracellular metabolites.

Alterations in protein acetylation after starvation

Starvation of mice reduces the overall level of protein acetylation in the heart and in the muscle,[21,26] a phenomenon that is related to the known capacity of starvation to deplete acetyl-CoA[21] and to activate the deacetylase activity of sirtuins.[27,28] Therefore, we investigated the effects of starvation on protein acetylation levels by immunofluorescence staining of permeabilized and fixed leukocytes with an antibody specific for protein
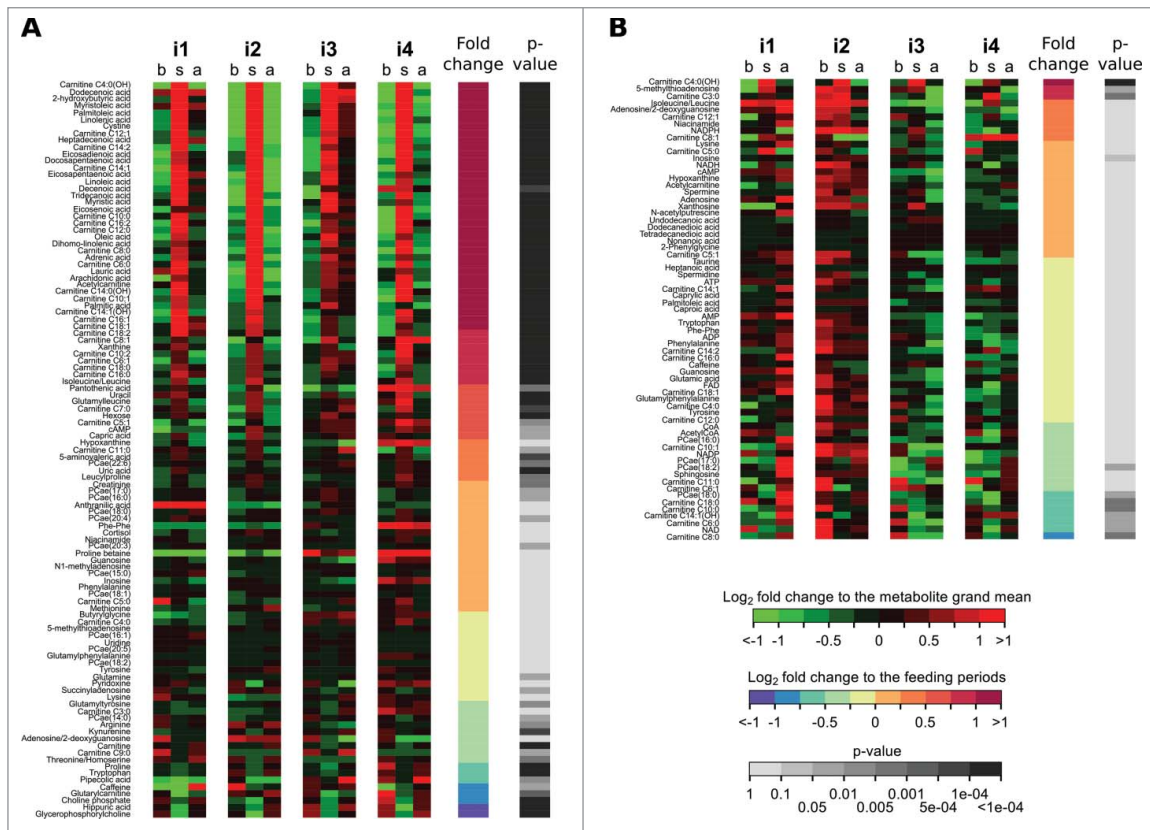
Figure 1. Metabolomic changes induced by starvation in the plasma and circulating leukocytes from healthy volunteers. Data are shown for 4 distinct individuals (numbered consecutively as i1 to i4) before (b), during (s) and after (a) starvation. For each volunteer, fasting blood was drawn on 3 consecutive d one wk before the starvation period (b), on d 1, 2, 3 and 4 of the starvation period (s), as well as one wk later, again on 3 consecutive d (a). Metabolomic analyses were performed on the plasma (A) and the intracellular metabolome of leukocytes (B). Note that only metabolites that vary by a factor of > 1.5 upon starvation have been listed.
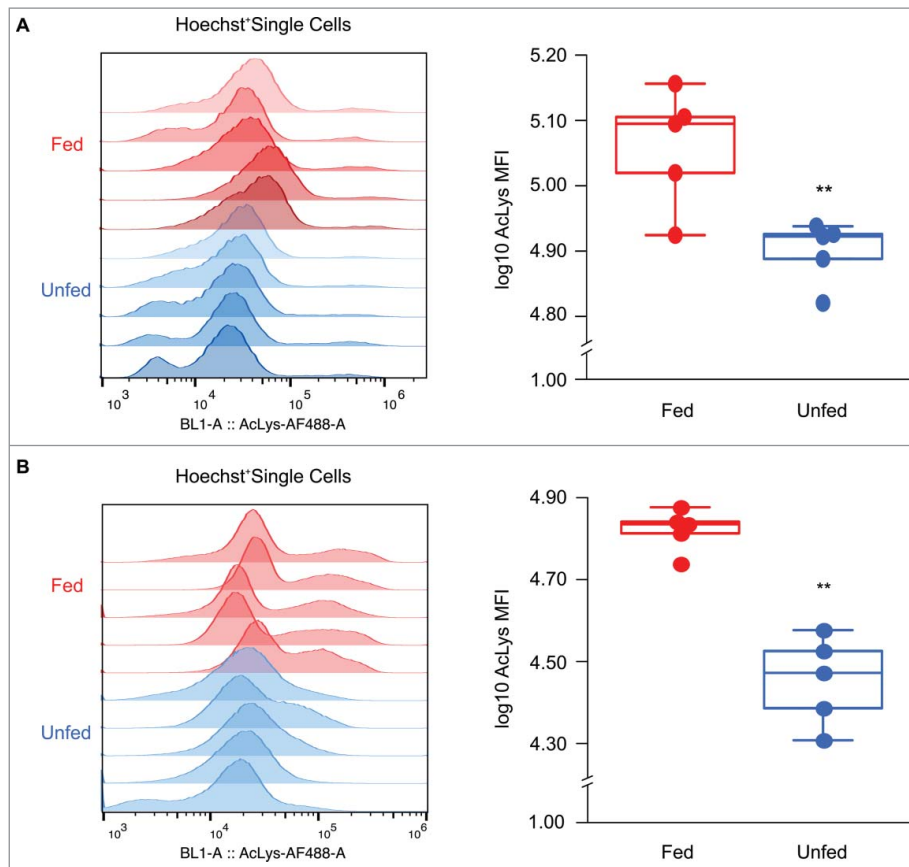
Figure 2. Metabolomic changes induced by a 48-h starvation period in the plasma and circulating leukocytes from mice. Data are shown for 5 individual mice for the plasma (A) and the intracellular metabolome of leukocytes (B). Note that only metabolites that vary by a factor of > 1 between fed control mice and starved mice have been listed.

containing acetylated lysine residues. Cytofluorometric analyses revealed that starvation caused a significant reduction in the levels of protein acetylation in circulating white blood cells from mice (Fig. 3A) and in human leukocytes (starting after 24-h fasting) upon starvation (Fig. 3B).

Next, we sought to investigate whether the starvation-induced deacetylation observed in mouse white blood cells would equally affect all leukocyte subpopulations and whether it would concern both the cytoplasmic and the nuclear compartments of the cells. For this, cells were first subjected to cell surface staining of the leukocyte marker PTPRC/CD45, then fixed or permeabilized to visualize acetylated proteins, and finally subjected to cytofluorometric analysis in an Amnis Image Stream® apparatus. This procedure, which combines PTPRC/CD45 staining and side scatter intensity (SSC) allowed us to distinguish major peripheral blood mononuclear subtypes, in accord with published findings[29-31] (Fig. S2). Counterstaining with the chromatin dye Hoechst 33342 allowed defining the nucleus as an area of interest, contrasting with the extranuclear (= cytoplasmic) area. Hence, the intensity of the immunostaining revealing protein acetylation could be independently determined for the nucleus and the cytoplasm on a single-cell basis for each major leukocyte subtype, including lymphocytes, monocytes, and neutrophil, eosinophil and basophil granulocytes (Fig. 4A). Importantly, starvation of mice significantly reduced protein acetylation in all cell types, both in nuclei and in the cytoplasm (Fig. 4B-D). Hence,

starvation causes an important, easily detectable protein deacetylation in mouse leukocytes.

Assessment of autophagic markers after starvation

Because protein deacetylation triggers autophagy, we next determined whether starvation-induced protein deacetylation would correlate with the manifestation of autophagy.[21,22,32] For this, we first performed a series of immunoblots to detect the lipidation of MAP1LC3B/LC3B (microtubule-associated protein 1 light chain 3 β), knowing that the autophagy-associated, covalent linkage of LC3B to phosphatidylethanolamine causes an increase in its electrophoretic mobility (the so-called LC3B-I→LC3B-II conversion).[33] In addition we measured the autophagy-dependent degradation of SQSTM1/p62, a receptor and scaffold protein interacting with LC3 and ubiquitinated proteins (through a specific LC3-interacting region [LIR] and ubiquitin-associated [UBA] domain, respectively).[34,35] Although stimuli able to activate autophagy rapidly induce SQSTM1/p62 degradation, a prolonged autophagy activation (as mediated by protracted fasting) may lead to a restoration of SQSTM1/p62 expression levels, hence complicating data interpretation.[36] Surprisingly, there were no signs of increased LC3B lipidation in leukocytes from starved mice, although protein levels of the autophagic substrate SQSTM1/p62 decreased (Fig. 5A, D, G) (possibly suggesting an accelerated autophagic flux).[16] Importantly hepatocytes from the same mice did exhibit a consistent increase in lipidated LC3B form and a

Figure 3. Reduction of lysine acetylation after starvation in murine and human leukocytes. (A) Representative cytofluorometric profiles (left panel) and quantification (boxplots, right panels) of Hoechst[+] murine leukocytes stained with an antibody specific for proteins containing acetylated lysine residues and detected by flow cytometry. Five mice per condition (fed *vs.* 48 h unfed) are shown. (B) Representative profiles (left panel) and quantification (boxplot, right panel) of Hoechst[+] human leukocyte acetylation. Profiles from 5 healthy volunteers (fed versus 24 h unfed) are depicted. Asterisks indicate significant differences. [**]p <0.01(unpaired *t* test). MFI, mean fluorescence intensity.

decrease in SQSTM1/p62 (Fig. 5B, E, H). We next sought to determine autophagic flux[16] by inhibiting the final steps of autophagy using intraperitoneal leupeptin injections.[37,38] In conditions in which mice received leupeptin during the last 2 h of the experiment, starvation did cause LC3B lipidation, both in leukocytes (Fig. 5A, D, G) and hepatocytes (Fig. 5B, E, H). No signs of enhanced autophagy-associated lipidation were detected in leukocytes from human subjects after starvation for periods as long as 4 d (Fig. 5C, F, I). However, ex vivo culturing of leukocytes from 24-h starved individuals for as little as 1 h allowed us to detect autophagy activation in these conditions, as suggested by enhanced LC3-II formation (both in the absence and presence of leupeptin) and SQSTM1/p62 elimination (in the absence of leupeptin) (Fig. 5J, K, L).

In the next step, we determined whether starvation of mice would stimulate autophagic flux in any of the circulating leukocyte subpopulations. For this, we stained leukocytes first with a PTPRC/CD45-specific antibody (revealed as a red fluorescence), then permeabilized and fixed the cells, stained them with an antibody specific for LC3B (revealed as a green fluorescence), and counterstained them with Hoechst 33342 to visualize the nuclei (blue fluorescence). As already demonstrated in a previous study[39] in standard conditions, leukocytes from starved mice failed to manifest an increase in the number of cytoplasmic LC3B^{+} puncta per cell. However, when leupeptin was systemically injected 2 h before recovery of blood samples,

starvation did cause an increase in the LC3B^{+} dots that could be readily detected by visual inspection (Fig. 6A) and that occurred consistently in all leukocyte subpopulations from starved mice (Figs. S3 and S4). Systematic analyses designed to define optimal thresholds to distinguish cells with low and high numbers of LC3B^{+} puncta (Fig. 6B), followed by statistical calculations (Fig. 6C) revealed that starvation induced a (leupeptin-revealed) increase in LC3B^{+} dots in all major leukocyte subpopulations including lymphocytes, monocytes and distinct granulocyte subsets. Similarly, photo-cytofluorimetric analysis of ex vivo cultured human leukocytes from 24-h starved human volunteers revealed an activation of autophagic flux (as measured by incubation for 1 h with leupeptin) compared with their fed counterparts. At difference with the mice experiments, we found that only neutrophils (representing the most abundant population of circulating leukocytes in humans, Fig. 7A) responded to fasting with an increased number of LC3B^{+} puncta (Fig. 7B). Altogether, these findings reveal that nutrient deprivation does stimulate autophagy flux in circulating leukocytes from mice and in cultured neutrophils from fasted human volunteers.

Discussion

Starvation induces major changes in the plasma metabolome that can be readily detected by mass spectrometry-based
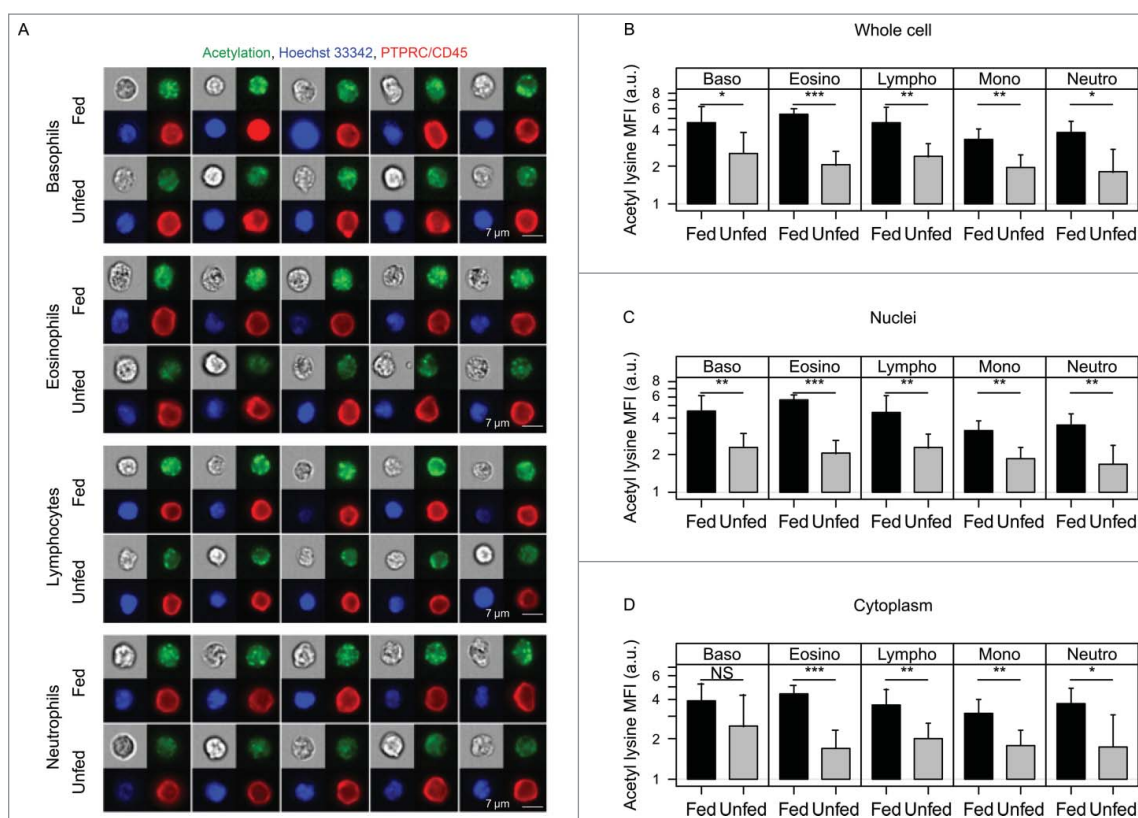
Figure 4. Reduction in the lysine acetylation level in mouse leukocytes after starvation. (A) Five images of representative cells from distinct leukocyte subpopulations, extracted from fed and unfed mice, are shown. Cells were stained with an antibody specific for proteins containing acetylated lysine residues and detected by multispectral imaging flow cytometry. (B-D) Quantification of acetylation levels in fed control mice versus unfed mice. Results are shown for whole cells (B), as well as for the areas of interest overlapping with nuclear Hoechst 33342 staining (C) or outside of the nucleus (D). Values are the mean of 5 mice ± SD. Asterisks indicate significant (unpaired Student t test) differences. $^*p<0.05$; ** p<0.01; ***p <0.001. a.u., arbitrary units; MFI, mean fluorescence intensity.

metabolomics, both in mice (after starvation for 48 h) and in humans (after starvation for 2–4 d). These alterations mainly consist in an increase in free fatty acids and/or different species of acylcarnitines, reflecting lipolysis during the mobilization of endogenous fat stores.[40,41] Importantly, analysis of gene expression profile in white blood cells from human volunteers subjected to 48-h fasting also revealed a PPARA (peroxisome proliferator activated receptor α)-dependent increase in fatty acid β-oxidation genes (starting 24 h after nutrient deprivation), therefore confirming our findings.[42] Notably, fasting also resulted in a prominent increase in the levels of the oxidized amino acid cystine, a condition that has been previously associated with physical exercise.[43] An intriguing possibility is that cystine would be absorbed from the blood stream by various organs (including the liver) and reduced in the cells; this reaction would then lead to the generation of H_2S, a gas that is essential for the beneficial effects of caloric restriction.[44] Collectively, these changes in the plasma metabolome constitute a convenient parameter to verify the compliance of human volunteers with the self-imposed starvation regimen. In sharp contrast to the plasma, the metabolome of circulating leukocytes underwent rather minor changes in the same conditions, underscoring the capacity of homeostatic mechanisms to maintain intracellular homeostasis in conditions of a changing extracellular environment.[45,46]

As reported for other mouse organs (such as the myocardium and the gastrocnemius muscle),[21] circulating leukocytes from mice manifested a sizeable reduction in protein acetylation that was detectable in all leukocyte subpopulations, both in the cytoplasmic and in the nuclear compartments. Nonetheless, this deacetylation was not accompanied by a significant drop in acetyl-CoA or by an increase in the concentration of free nicotinamide adenine dinucleotide (NAD) (that would cause the activation of the deacetylase activity of sirtuins).[20] Hence, alterations in the intracellular metabolome cannot account for the reduced acetylation of leukocyte proteins. One possible explanation for the reduced protein acetylation may reside in the neuro-endocrine response to starvation, which includes a reduction in IGF1 (insulin like growth factor 1) and an increase in its antagonist, IGFBP (insulin like growth factor binding protein).[47,48] The starvation-induced reduction in IGF1 bioavailability would reduce the AKT1 (AKT serine/threonine kinase 1)-dependent activity of the acetyl-CoA-generating enzyme ACLY (ATP citrate lyase).[49] If a reduced flux in acetyl-CoA production was linked to immediate deacetylation, then the acetate generated as a result of histone deacetylation would cause an immediate increase in free acetate, which in turn would constitute a source for acetyl-CoA, hence maintaining stable acetyl-CoA levels.[50,51] Nonetheless, this hypothetical conjecture requires further exploration.

In line with fasting mice, human leukocytes manifested signs of major protein deacetylation, starting at 24 h post-fasting regimen. Altogether, these findings highlight protein
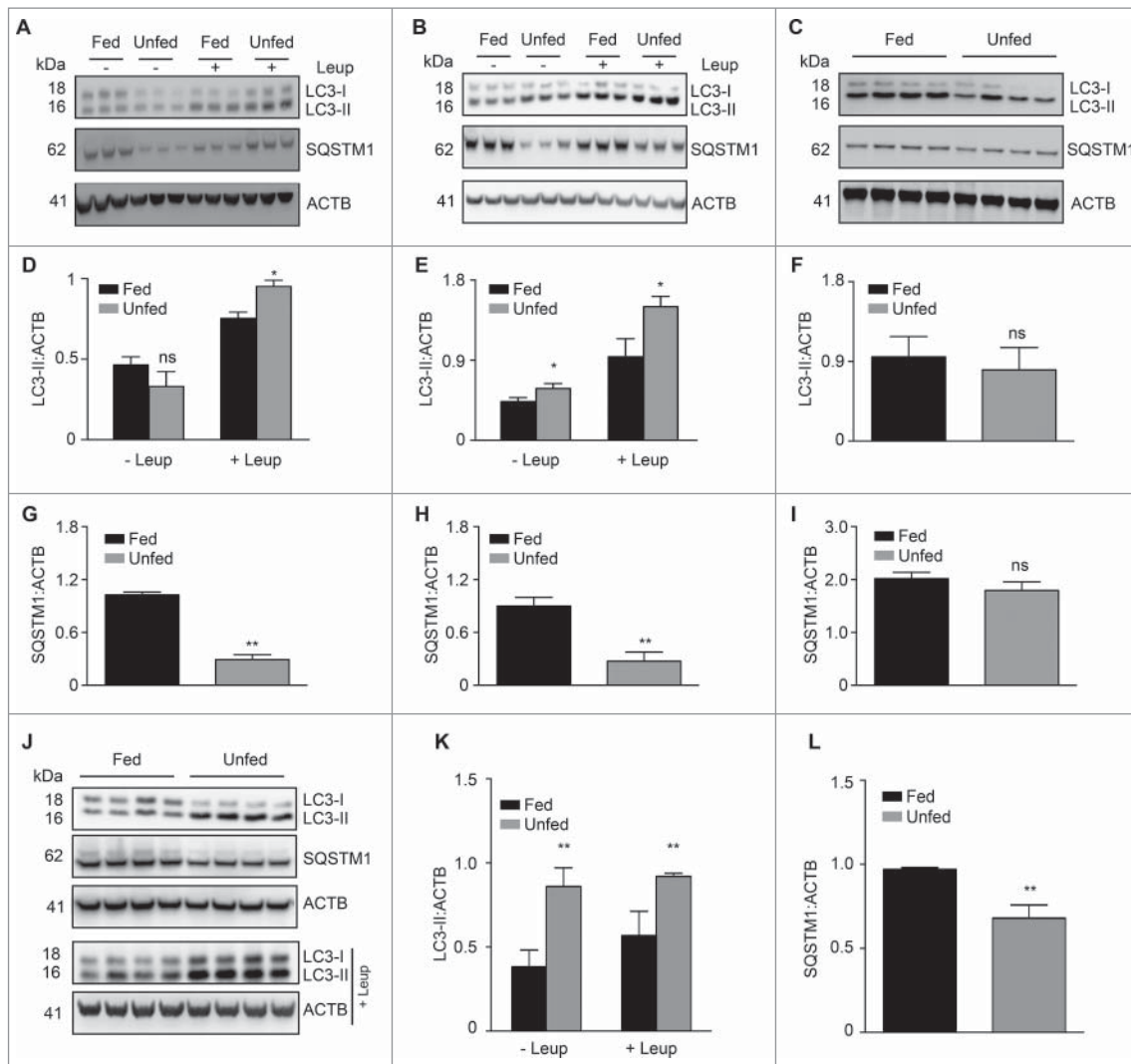
Figure 5. Autophagy flux detection in circulating leukocytes from mice and humans. (A, B) Representative immunoblots of LC3B and SQSTM1/p62 from mouse leukocytes (A) and liver (B) that were fed normally or starved for 48 h (unfed) and were optionally injected with the protease inhibitor leupeptin (Leup) 2 h before recovering blood and organs. Three mice per condition are shown. Autophagy was evaluated as LC3-I to LC3-II conversion (quantified in (D)and E) and SQSTM1/p62 degradation (quantified in (G)and H). Results from one representative experiment (n = 3) are expressed as mean ± SD. *p < 0.05; **p < 0.01 (unpaired t test); ns, nonsignificant. (C) Failure in detecting autophagy in leukocytes from individuals that had been starved for 48 h. Four healthy volunteers per condition (fed versus unfed) are shown. Quantification of LC3-II lipidation and SQSTM1/p62 are illustrated in (F) and (I), resulting in nonsignificant (ns) differences (paired t-test). (J) Representative immunoblots of LC3B and SQSTM1/p62 from fed or 24-h starved human leukocytes cultured for 1 h ex vivo in the absence or presence of leupeptin are depicted. One representative experiment (n = 2) with 4 healthy volunteers per condition is shown. Evaluation of LC3-II formation and SQSTM1/p62 degradation (quantified in (K)and L) shows enhanced autophagic flux in starved individuals. **p < 0.01 (unpaired t test).

deacetylation as a reliable biochemical marker of nutritional stress status. It may be interesting to investigate protein acetylation in conditions beyond those that can be investigated by voluntary nutrient deprivation, for instance in cachectic cancer patients or in individuals affected by anorexia.

Although starvation induced a significant level of protein deacetylation in all leukocyte subpopulations in mice, no concomitant signs of increased autophagy could be detected (measured as LC3B lipidation or immunofluorescence-detectable LC3B puncta) unless the final steps of autophagy were blocked by means of the protease inhibitor leupeptin. Nonetheless, levels of the autophagic substrate SQSTM1/p62 decreased in these conditions, hence suggesting that this protein can be used as marker of enhanced autophagic flux in leukocytes. After injection of leupeptin, 2 h before termination of the starvation experiments (which lasted a total of 48 h), a major and

significant increase in LC3B lipidation (detectable by immunoblot) or LC3B$^+$ dots (detectable by immunofluorescence) became apparent. Sophisticated cytofluorometry accompanied by microphotography of each individual leukocyte, followed by computer-assisted image analyses, indicated that autophagic flux (revealed by leupeptin treatment) was induced by starvation in all leukocyte subpopulations. In line with these observations, ex vivo culture of white blood cells from human volunteers allowed us to measure autophagic flux (both in the presence or absence of an inhibitor of lysosomal degradation); autophagy already became detectable in neutrophils 24 h after the beginning of the fasting regimen, possibly underlying a decisive contribution of autophagy in the mobilization of energy stores[42] observed at early time points. Contrary to mice, in which all leukocyte subpopulations exhibited signs of enhanced autophagic flux, only neutrophils from healthy volunteers presented an increased number of LC3B$^+$ puncta, in
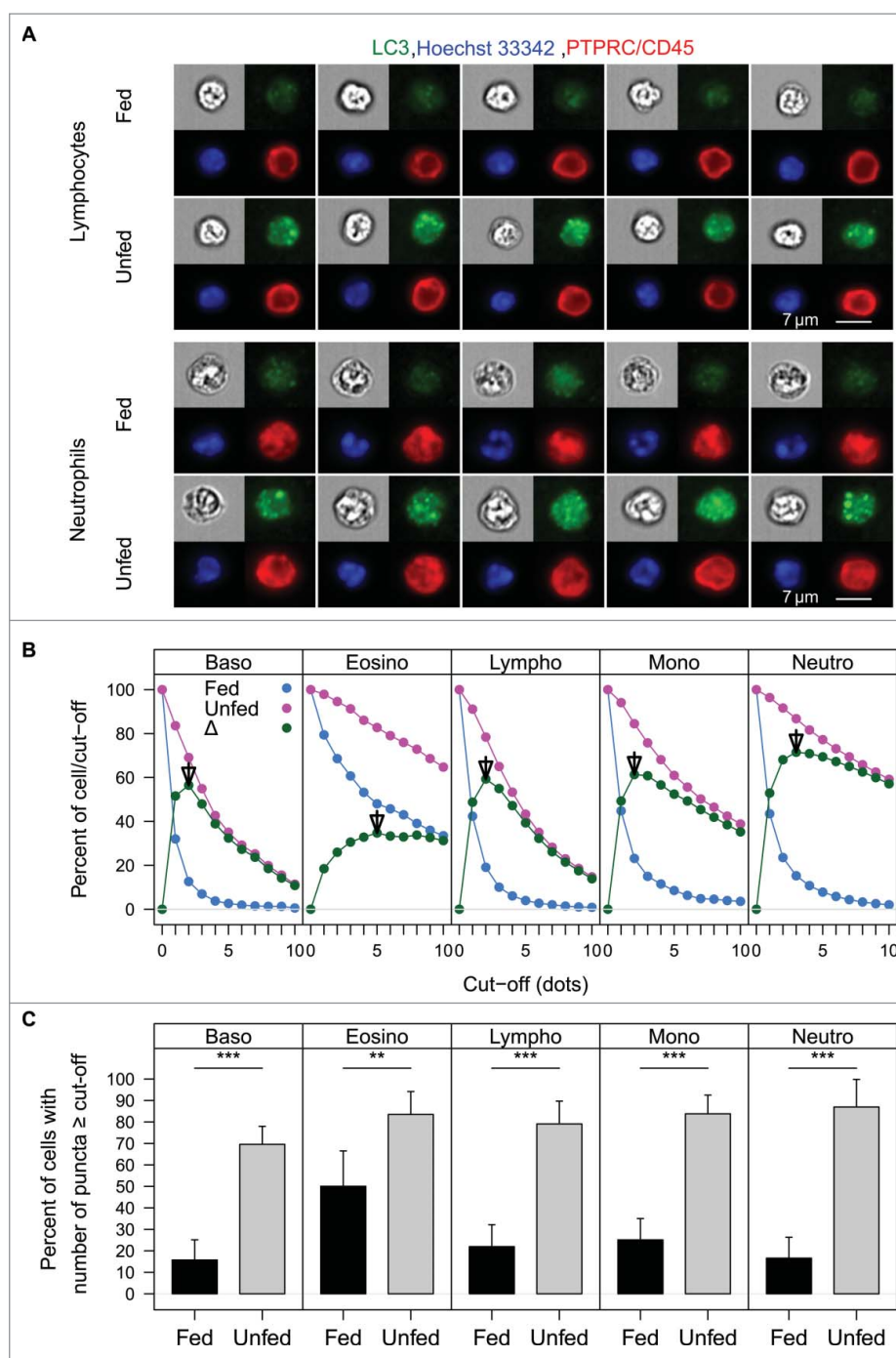
Figure 6. Induction of autophagy in circulating mouse leukocytes upon starvation, as revealed by leupeptin treatment. Mice were fed normally or kept under nutrient-free (unfed) conditions for 48 h. Leupeptin was injected 2 h before termination of the experiment, and blood was drawn. (A) Representative staining of lymphocytes and neutrophils to visualize cytoplasmic LC3B puncta in cells from unfed mice. (B) Determination of the optimal cut-off value to distinguish cells with normal or induced autophagy (as measured by counting the number of LC3B puncta per cell) between fed and unfed mice for each leukocyte population. The green line indicates differences in number of dots between fed and unfed conditions. Optimal cut-offs are indicated with arrows. (C) The percentage of leukocyte subpopulations from fed or unfed mice that contained more LCB puncta per cell than the cut-off value determined in (B) was determined for each individual mouse. Results are means ± SD of 5 animals per group. **p<0.01; ***p<0.001 (unpaired Student *t* test).

line with previous findings showing autophagy activation in this population.[54,55] In addition, it has been previously demonstrated that detection of autophagy in neutrophils can be used to monitor autophagic flux at the whole body level in the context of pathological settings.[56] At present, the reasons for this discrepancy between mice and humans with respect to autophagy induction in all leukocyte subpopulation and neutrophils only, respectively, are elusive. This difference may be related to the intensity of the autophagy-inducing protocol between the 2 species, as well as to the fact that leupeptin was injected in vivo into mice but only used in vitro in the human context. Nonetheless, this work reveals that procedures aiming to measure autophagic flux (and protein deacetylation) in human and murine leukocytes are suitable to follow autophagy activation at the whole body level and offer a reliable portrait of the nutritional status of the entire organism.
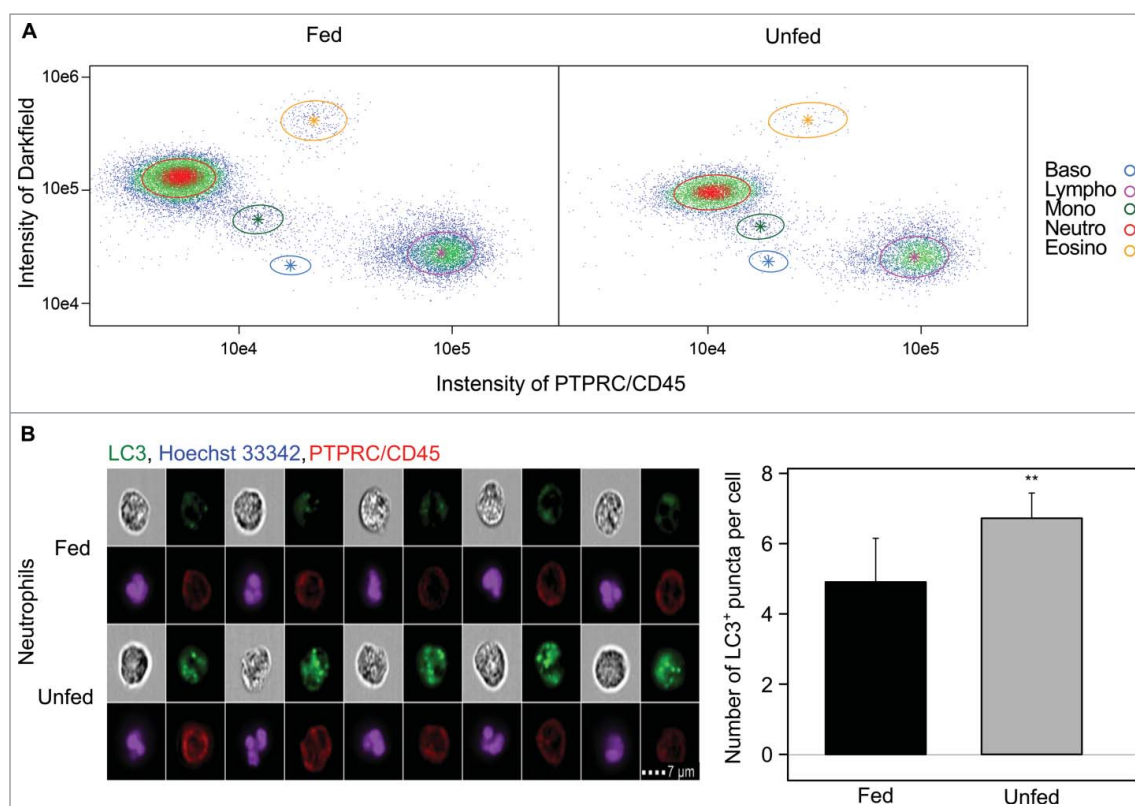
Figure 7. Induction of autophagy in cultured human neutrophils upon nutrient starvation. (A, B) Leukocytes from fed or 24-h starved human leukocytes were isolated and cultured for 1 h in the presence of leupeptin. (A) Representative cytofluorometric pictograms of circulating leukocytes are depicted for one fed (left panel) and one unfed (right panel) volunteer and show that neutrophils are the majority population among human leukocyte subtypes. (B) Representative staining of neutrophils to visualize cytoplasmic LC3B puncta in cells from fed versus starved individuals (quantified in the graph). Results are expressed as means ± SD of 5 human volunteers per group ** $p < 0.01$ (unpaired Student t test).

Materials and methods

Starvation regimen

Six-wk-old female C57BL/6 mice were kept in standard conditions or were left for 48 h in the absence of nutrients (though with ad libitum access to drinking water) following standard procedures. [19] After this period, animals were anesthetized and blood was drawn by cardiac puncture, followed by euthanasia. Optionally, mice received i.p. injection of 30 mg/kg leupeptin (Sigma Aldrich, L2884) 2 h before blood collection. Experiments were performed in compliance with the EU Directive 63/2010, and protocols (reference number 03981.02) were approved by the local ethics committee (C2EA n. 5, registered at the French Ministry of Research). Nine healthy human volunteers (age 24–54, 5 males, 4 females, all without any known past or present pathology and a normal body mass index of 20–25) agreed to engage in a zero-calorie diet (with water, tea and coffee ad libitum) for 4 consecutive d. Heparin blood was drawn every morning between 9 and 9:30 a.m. during the starvation period, as well as on 3 consecutive d (without prior breakfast) 1 wk before and 1 wk after the starvation period. Freshly isolated human leukocytes were incubated for 1 h at 37°C in Dulbecco's modified Eagle medium supplemented with 10% fetal bovine serum in the presence or absence of 100 μM leupeptin.

Preparation of leukocytes and plasma

After blood drawing, 500 μL total blood were diluted in 5 mL red blood cell lysis buffer (BioLegend, 420301) for 10 min at room temperature and washed twice in phosphate-buffered saline (PBS; Thermo Fisher Scientific, 10010023). For immunoblotting, white cells were lysed in 50 μL radio immunoprecipitation assay (RIPA) buffer. For cytofluorimetric assay, cells were fixed in 4% paraformaldehyde and processed as described below. Alternatively, cells were subjected to metabolomics analyses. For this purpose, cells were transferred into 1.5 mL microcentrifuge tubes, centrifuged (2 min at 1000 g, 4°C) and then washed with ice cold PBS. Washing and centrifugation were repeated once. Cell pellets were then resuspended in 100 μL of ice-cold hypo-osmotic buffer (1 M HEPES, 1 M EDTA, pH 7.4), vortexed and heated at 100°C for 5 min. Samples were incubated in liquid nitrogen for 5 min and thawed on ice. This cycle was repeated twice. Samples were kept for 1 h at −20°C and centrifuged at 4°C for 15 min at 13000 g. Supernatants were transferred into ultra-high performance liquid chromatography (UHPLC) vials and injected into the LC-MS or kept at −80°C until injection.

For plasma preparation, a volume of 100 μl of plasma was mixed with a cold solvent mixture (acetonitrile:2-propanol: water, 3:3:2, −20°C), in a 1.5 mL polypropylene microcentrifuge tube, vortexed and centrifuged (10 min at 15000 g, 4°C). The supernatant was collected in microcentrifuge tubes and evaporated at 40°C in a pneumatically assisted concentrator (Techne DB3, *Staffordshire*, *UK*). Methanol (300 μL) was added to the dried extract, which was further split into 2 fractions of 150 μl: one as a back up and one for LC-MS analysis. After evaporation, the dried extracts were resuspended in

300 μL of MilliQ water, centrifuged (10 min at 15000 g, 4°C) and aliquoted in 3 microcentrifuge tubes. Aliquots were transferred to UHPLC vials and injected in the LC-MS or kept at −80°C until injection.

Untargeted metabolomics analysis of intracellular metabolites by UHPLC coupled to a quadrupole-time of flight (QTOF) mass spectrometer

Profiling of intracellular metabolites was performed on a RRLC 1260 system (Agilent Technologies, Waldbronn, Germany) coupled to a QTOF 6520 (Agilent Technologies, Waldbronn, Germany) equipped with an electrospray source operating in full scan mode, from 50 to 1000 Da for both positive and negative ionization modes. The gas temperature was set at 350°C with a gas flow of 12 L/min. The capillary voltage was set at 3.5 kV, and the fragmentor at 120 V. Two reference masses were used to maintain the mass accuracy during analysis: m/z 121.050873 and m/z 922.009798 in positive mode and m/z 112.985587 and m/z 980.016375 in negative mode. Samples (10 μL) were injected on a SB-Aq column (100 mm × 2.1 mm, particle size 1.8 μm) from Agilent Technologies (Waldbronn, Germany), protected by a guard column XDB-C18 (5 mm × 2.1 mm, particle size 1.8 μm) and heated at 40°C. The gradient mobile phase consisted of water with 0.2% acetic acid (A) and acetonitrile (B). The flow rate was set at 0.3 ml/min. The initial condition was 98% phase A and 2% phase B. Molecules were then eluted using a gradient from 2% to 95% phase B in 7 min. The column was washed using 95% mobile phase B for 3 min and equilibrated using 2% mobile phase B for 3 min. The autosampler was kept at 4°C. Biological samples are randomized alongside 6 to 7 quality control (QC) samples that were assembled by pooling all experimental samples and that were injected at regular intervals.

Targeted analysis of intracellular metabolites by UHPLC coupled to a triple quadrupole (QQQ) mass spectrometer

Targeted analysis was performed on a RRLC 1260 system (Agilent Technologies, Waldbronn, Germany) coupled to a Triple Quadrupole 6410 (Agilent Technologies, Waldbronn, Germany) equipped with an electrospray source operating in positive mode. The gas temperature was set at 350°C with a gas flow of 12 l/min. The capillary voltage was set at 3.5 kV. Samples (10 μL) were injected on a Column Zorbax Eclipse XDB-C18 (100 mm × 2.1 mm, particle size 1.8 μm) from Agilent technologies (Waldbronn, Germany), protected by a guard column XDB-C18 (5 mm × 2.1 mm, particle size 1.8 μm) and heated at 40°C. The gradient mobile phase consisted of water with 2 mM DBAA (dibutylamine-acetic acid buffer) (A) and acetonitrile (B). The flow rate was set at 0.2 mL/min, and the gradient as follows: initial condition of 90% phase A and 10% phase B was maintained for 4 min and then from 10% to 95% phase B over 3 min. The column was washed using 95% mobile phase B for 3 min and equilibrated using 10% mobile phase B for 3 min. The autosampler was kept at 4°C. Biological samples were randomized alongside 6 to 7 QC samples.

Compound Name	Precursor Ion	Product Ion	Fragmentor	Collision Energy
Acetyl CoA	810.1	428	180	20
Acetyl CoA	810.1	303.1	180	28
FAD	786	439	20	20
FAD	786	348	20	20
CoA	768.1	261.2	180	32
NADPH	746	729	200	10
NADPH	746	136	200	40
NADP	744.1	604.1	200	20
NADP	744.1	136	200	50
NADH	666	649	190	10
NADH	666	514	190	20
NAD	664.1	428.1	190	24
NAD	664.1	136	190	50
ATP	508	136	45	40
ADP	428.2	348.1	172	16
ADP	428.2	136	172	28
AMP	348.2	136	99	20
Adenosine	268.1	136	100	16
Adenosine	268.1	119	100	50

MRM transitions are reported in Table S2.

Signal processing and data analysis of metabolomics data

Metabolomics profiles generated by LC-QTOF were processed using an in-house set of tools for converting the raw-MS data into a matrix compatible with the statistical analyses and for annotating the resulting peaks. Out of the 3139 features quantified in the human and mouse data sets, we only present data from nonredundant and identified peaks (Fig. S1). At the exception of most acylcarnitines and fatty acids, for which retention time is inferred from their respective number of carbons and insaturations, metabolite identities were confirmed by matching both accurate mass (17 ppm) and retention time (0.2 min) to those of standards of pure compounds measured in the same analytical conditions. For each data set, metabolites that contained more than 3/8 (mice/human respectively) missing values or exhibited a 95% signal-to-blank sample ratio lower than 5 or a coefficient of variation determined in the QC samples greater than 20% were excluded from the corresponding data set. The final metabolomics matrix comprised 163 compounds: 133 (plasma: 107; leukocyte: 65) for human plasma and 112 (plasma: 107; leukocyte: 56) for the mouse specimens. All statistical analyses and data representation were performed on pre-processed, log-basis 2 transformed and imputed metabolomics data[24] and reported as such without back-transformation. Moderated statistics adhering to the characteristics of the experimental design were used for differential analysis.[25] Fold changes and associated p-values are reported in Supplemental Table alongside metabolite name, HMDB (Human Metabolome Database) and KEGG (Kyoto Encyclopedia of Genes and Genomes) identities for facilitating data exchange.

Immunoblots

For immunoblotting, proteins extracted from isolated leukocytes and mouse liver were separated on 4–12% bis-tris acrylamide (ThermoFisher Scientific, NP0321) and electrotransferred to PVDF membranes (Bio-Rad, 1620177). Membranes were then horizontally sliced into different parts according to the molecular weight of the protein of interest to allow simultaneous detection of different antigens within the

same experiment. Nonspecific binding sites were saturated by incubating membranes for 1 h in 0.05% Tween 20 (Euromedex, 2001-C) (v:v in TBS [Euromedex, ET220-B]) supplemented with 5% nonfat powdered milk (w:v in TBS), followed by an overnight incubation with primary antibodies specific for LC3B (Cell Signaling Technology, 2775) and SQSTM1/p62 (Abnova, H00008878-M01). Development was performed with appropriate horseradish peroxidase-labeled secondary antibodies (Thermo Fisher Scientific, A16110 and 31430) plus the Super-Signal West Pico chemoluminescent substrate (Thermo Fisher Scientific, 34080). Anti-ACTB/beta-actin (Abcam, ab49900) was used to control equal loading of lanes.

Immunofluorescence staining

For LC3-II detection, isolated leukocytes were fixed in 4% paraformaldehyde for 30 min at 37°C. Fixed cells were permeabilized by means of 50% methanol, and nonspecific sites were blocked with bovine serum albumin (2%; Sigma Aldrich, A2153) in PBS. Cells were then incubated overnight with an anti-LC3B antibody and for 1 h at room temperature with Alexa-Fluor® 488-conjugated secondary antibody (Thermo Fisher Scientific, A-11008) and Hoechst 33342 (Thermo Fisher Scientific, H1399). For acetylation measurements, leukocytes were fixed with 4% paraformaldehyde for 1 h at room temperature, blocked with 2% bovine serum albumin in PBS and incubated overnight with anti-acetylated lysine antibody (Cell Signaling Technology, 9441) and for 1 h at room temperature with an Alexa-Fluor® 488 conjugated secondary antibody. Leukocyte immunophenotyping was obtained through staining of human and murine white blood cells with anti Alexa Fluor® 647 anti-mouse PTPRC/CD45 antibody (BioLegend, clone 30-F11) or Alexa Fluor® 647 anti-human PTPRC/CD45 antibody (BioLegend, clone HI30).

Cytofluorometric analysis

Multispectral imaging flow cytometry was performed on an AMNIS ImageStream X Mark II equipped with 375-, 488-, 561-, and 642-nm lasers using the 60x magnification lens. The autosampler was used for acquisition and only Hoechst$^+$ events were recorded. The analysis was done with IDEAS software v6.1. Only focused events were included in the analysis, using the gradient RMS feature of bright field images. Saturated signals in fluorescence channels and raw centroid X cut objects were eliminated. Singlets were then gated on aspect ratio vs area of bright field and leukocyte subpopulations were gated on a pictogram indicating the intensity of PTPRC/CD45 staining versus dark field. A morphology mask was applied on the Hoechst 33342-stained part of the cells to identify the nuclear area, whereas the cytoplasm was defined as the extranuclear area delimited by the nuclear area (plus one pixel to erode the mask) and the outer limit of the cell defined by bright field. The intensity of acetyl lysine staining was quantified within these 2 masks and the entire cell. Values were exported to text files for R analyses. Flow cytometric analysis of acetylation was performed on an Attune Ntx Flow Cytometer (Thermo Fisher Scientific) equipped with 405- and 488-nm lasers.

Statistical analyses

Statistical analyses were performed by R software. Leukocytes were manually clustered to define basophiles, eosinophils, lymphocytes, monocytes and neutrophils based on their dark field and PTPRC/CD45 staining intensity (Fig. S2). For each described cell type an unpaired t test was performed between fed vs unfed animals. In the case of lysine acetylation the means of log10 intensity of staining of each control replicate (5) were compared against the means of log10 intensity of staining of each starved (5) mouse. For the quantification of LC3B puncta, the best cut-off was defined as the number of puncta for which the proportion of each cell type showed the greatest difference between fed and unfed mice. The proportion of each cell type with several dots equal to or higher than the cut-off for each replicate was compared by means of an unpaired t test to evaluate differences between starved and control animals.

Abbreviations

AKT1	AKT serine/threonine kinase 1
EP300	E1A binding protein p300
IGF1	insulin-like growth factor 1
IGFBP	insulin like growth factor binding protein
LIR	LC3-interacting region
MAP1LC3B/LC3B	microtubule-associated protein 1 light chain 3 β
NAD	nicotinamide adenine dinucleotide; SQSTM1/p62, sequestome1
SSC	side scatter
UBA	ubiquitin-associated
UHPLC	ultra-high performance liquid chromatography

Disclosure of potential conflicts of interest

No potential conflicts of interest were disclosed.

Funding

References

[1] Mizushima N, Klionsky DJ. Protein turnover via autophagy: implications for metabolism. Annu Rev Nutr 2007; 27:19-40; PMID:17311494; http://dx.doi.org/10.1146/annurev.nutr.27.061406.093749

[2] He C, Klionsky DJ. Regulation mechanisms and signaling pathways of autophagy. Annu Rev Genet 2009; 43:67-93; PMID:19653858; http://dx.doi.org/10.1146/annurev-genet-102808-114910

[3] Levine B, Mizushima N, Virgin HW. Autophagy in immunity and inflammation. Nature 2011; 469:323-35; PMID:21248839; http://dx.doi.org/10.1038/nature09782

[4] Shen HM, Mizushima N. At the end of the autophagic road: an emerging understanding of lysosomal functions in autophagy. Trends Biochem Sci 2014; 39:61-71; PMID:24369758; http://dx.doi.org/10.1016/j.tibs.2013.12.001

[5] Galluzzi L, Pietrocola F, Bravo-San Pedro JM, Amaravadi RK, Baehrecke EH, Cecconi F, Codogno P, Debnath J, Gewirtz DA, Karantza V, et al. Autophagy in malignant transformation and cancer progression. EMBO J 2015; 34:856-80; PMID:25712477; http://dx.doi.org/10.15252/embj.201490784

[6] Melendez A, Talloczy Z, Seaman M, Eskelinen EL, Hall DH, Levine B. Autophagy genes are essential for dauer development and lifespan extension in C. elegans. Science 2003; 301:1387-91.

[7] Tavernarakis N, Pasparaki A, Tasdemir E, Maiuri MC, Kroemer G. The effects of p53 on whole organism longevity are mediated by autophagy. Autophagy 2008; 4:870-3; PMID:18728385; http://dx.doi.org/10.4161/auto.6730

[8] Eisenberg T, Knauer H, Schauer A, Buttner S, Ruckenstuhl C, Carmona-Gutierrez D, Ring J, Schroeder S, Magnes C, Antonacci L, et al. Induction of autophagy by spermidine promotes longevity. Nat Cell Biol 2009; 11:1305-14; PMID:19801973; http://dx.doi.org/10.1038/ncb1975

[9] Morselli E, Maiuri MC, Markaki M, Megalou E, Pasparaki A, Palikaras K, Criollo A, Galluzzi L, Malik SA, Vitale I. Caloric restriction and resveratrol promote longevity through the Sirtuin-1-dependent induction of autophagy. Cell Death Dis 2010; 1:e10; PMID:21364612; http://dx.doi.org/10.1038/cddis.2009.8

[10] Bjedov I, Toivonen JM, Kerr F, Slack C, Jacobson J, Foley A, Partridge L. Mechanisms of life span extension by rapamycin in the fruit fly Drosophila melanogaster. Cell Metab 2010; 11:35-46; PMID:20074526; http://dx.doi.org/10.1016/j.cmet.2009.11.010

[11] Rubinsztein DC, Marino G, Kroemer G. Autophagy and aging. Cell 2011; 146:682-95; PMID:21884931; http://dx.doi.org/10.1016/j.cell.2011.07.030

[12] Lopez-Otin C, Blasco MA, Partridge L, Serrano M, Kroemer G. The hallmarks of aging. Cell 2013; 153:1194-217; PMID:23746838; http://dx.doi.org/10.1016/j.cell.2013.05.039

[13] Madeo F, Zimmermann A, Maiuri MC, Kroemer G. Essential role for autophagy in life span extension. J Clin Invest 2015; 125:85-93; PMID:25654554; http://dx.doi.org/10.1172/JCI73946

[14] Levine B, Kroemer G. Autophagy in the pathogenesis of disease. Cell 2008; 132:27-42; PMID:18191218; http://dx.doi.org/10.1016/j.cell.2007.12.018

[15] Klionsky DJ, Abdalla FC, Abeliovich H, Abraham RT, Acevedo-Arozena A, Adeli K, Agholme L, Agnello M, Agostinis P, Aguirre-Ghiso JA, et al. Guidelines for the use and interpretation of assays for monitoring autophagy. Autophagy 2012; 8:445-544; PMID:22966490; http://dx.doi.org/10.4161/auto.19496

[16] Klionsky DJ, Abdelmohsen K, Abe A, Abedin MJ, Abeliovich H, Acevedo Arozena A, Adachi H, Adams CM, Adams PD, Adeli K, et al. Guidelines for the use and interpretation of assays for monitoring autophagy (3rd edition). Autophagy 2016; 12:1-222; PMID:26799652; http://dx.doi.org/10.1080/15548627.2015.1100356

[17] Rubinsztein DC, Cuervo AM, Ravikumar B, Sarkar S, Korolchuk V, Kaushik S, Klionsky DJ. In search of an "autophagomometer". Autophagy 2009; 5:585-9; PMID:19411822; http://dx.doi.org/10.4161/auto.5.5.8823

[18] Ju JS, Varadhachary AS, Miller SE, Weihl CC. Quantitation of "autophagic flux" in mature skeletal muscle. Autophagy 2010; 6:929-35; PMID:20657169; http://dx.doi.org/10.4161/auto.6.7.12785

[19] Mizushima N, Yamamoto A, Matsui M, Yoshimori T, Ohsumi Y. In vivo analysis of autophagy in response to nutrient starvation using transgenic mice expressing a fluorescent autophagosome marker. Mol Biol Cell 2004; 15:1101-11; PMID:14699058; http://dx.doi.org/10.1091/mbc.E03-09-0704

[20] Imai S, Guarente L. NAD+ and sirtuins in aging and disease. Trends Cell Biol 2014; 24:464-71; PMID:24786309; http://dx.doi.org/10.1016/j.tcb.2014.04.002

[21] Marino G, Pietrocola F, Eisenberg T, Kong Y, Malik SA, Andryushkova A, Schroeder S, Pendl T, Harger A, Niso-Santano M, et al. Regulation of autophagy by cytosolic acetyl-coenzyme A. Mol Cell 2014; 53:710-25; PMID:24560926; http://dx.doi.org/10.1016/j.molcel.2014.01.016

[22] Madeo F, Pietrocola F, Eisenberg T, Kroemer G. Caloric restriction mimetics: towards a molecular definition. Nat Rev Drug Discov 2014; 13:727-40; PMID:25212602; http://dx.doi.org/10.1038/nrd4391

[23] Pietrocola F, Lachkar S, Enot DP, Niso-Santano M, Bravo-San Pedro JM, Sica V, Izzo V, Maiuri MC, Madeo F, Mariño G. Spermidine induces autophagy by inhibiting the acetyltransferase EP300. Cell Death Differ 2015; 22:509-16; PMID:25526088; http://dx.doi.org/10.1038/cdd.2014.215

[24] Kim H, Golub GH, Park H. Missing value estimation for DNA microarray gene expression data: local least squares imputation. Bioinformatics 2005; 21:187-98; PMID:15333461; http://dx.doi.org/10.1093/bioinformatics/bth499

[25] Ritchie ME, Phipson B, Wu D, Hu Y, Law CW, Shi W, Smyth GK. limma powers differential expression analyses for RNA-sequencing and microarray studies. Nucleic Acids Res 2015; 43:e47; PMID:25605792; http://dx.doi.org/10.1093/nar/gkv007

[26] Pietrocola F, Pol J, Vacchelli E, Baracco EE, Levesque S, Castoldi F, Maiuri MC, Madeo G, Kroemer G. Autophagy induction for the treatment of cancer. Autophagy 2016:12:1962-1964.

[27] Hariharan N, Maejima Y, Nakae J, Paik J, Depinho RA, Sadoshima J. Deacetylation of FoxO by Sirt1 Plays an Essential Role in Mediating Starvation-Induced Autophagy in Cardiac Myocytes. Circ Res 2010; 107:1470-82; PMID:20947830; http://dx.doi.org/10.1161/CIRCRESAHA.110.227371

[28] Longo VD. Linking sirtuins, IGF-I signaling, and starvation. Exp Gerontol 2009; 44:70; PMID:18638538; http://dx.doi.org/10.1016/j.exger.2008.06.005

[29] Fendl B, Weiss R, Fischer MB, Spittler A, Weber V. Characterization of extracellular vesicles in whole blood: Influence of pre-analytical parameters and visualization of vesicle-cell interactions using imaging flow cytometry. Biochem Biophys Res Commun 2016; 478:168-73; PMID:27444383; http://dx.doi.org/10.1016/j.bbrc.2016.07.073

[30] Samsel L, Dagur PK, Raghavachari N, Seamon C, Kato GJ, McCoy JP, Jr. Imaging flow cytometry for morphologic and phenotypic characterization of rare circulating endothelial cells. Cytometry B Clin Cytom 2013; 84:379-89; PMID:23554273; http://dx.doi.org/10.1002/cyto.b.21088

[31] Clark RT. Imaging flow cytometry enhances particle detection sensitivity for extracellular vesicle analysis; Nature Methods 2015; 12; PMID:27444383; http://dx.doi.org/10.1038/nmeth.3321

[32] Eisenberg T, Schroeder S, Andryushkova A, Pendl T, Kuttner V, Bhukel A, Mariño G, Pietrocola F, Harger A, Zimmermann A, et al. Nucleocytosolic depletion of the energy metabolite acetyl-coenzyme a stimulates autophagy and prolongs lifespan. Cell Metab 2014; 19:431-44; PMID:24606900; http://dx.doi.org/10.1016/j.cmet.2014.02.010

[33] Mizushima N, Yoshimori T. How to interpret LC3 immunoblotting. Autophagy 2007; 3:542-5; PMID:17611390; http://dx.doi.org/10.4161/auto.4600

[34] Bjorkoy G, Lamark T, Pankiv S, Overvatn A, Brech A, Johansen T. Monitoring autophagic degradation of p62/SQSTM1. Methods Enzymol 2009; 452:181-97; PMID:19200883; http://dx.doi.org/10.1016/S0076-6879(08)03612-4

[35] Komatsu M, Ichimura Y. Physiological significance of selective degradation of p62 by autophagy. FEBS Lett 2010; 584:1374-8; PMID:20153326; http://dx.doi.org/10.1016/j.febslet.2010.02.017

[36] Sahani MH, Itakura E, Mizushima N. Expression of the autophagy substrate SQSTM1/p62 is restored during prolonged starvation depending on transcriptional upregulation and autophagy-derived amino acids. Autophagy 2014; 10:431-41; PMID:24394643; http://dx.doi.org/10.4161/auto.27344

[37] Mofarrahi M, Guo Y, Haspel JA, Choi AM, Davis EC, Gouspillou G, Hepple RT, Godin R, Burelle Y, Hussain SN. Autophagic flux and

oxidative capacity of skeletal muscles during acute starvation. Autophagy 2013; 9:1604-20; PMID:23955121; http://dx.doi.org/10.4161/auto.25955

[38] Esteban-Martinez L, Boya P. Autophagic flux determination *in vivo* and ex vivo. Methods 2015; 75:79-86; PMID:25644445; http://dx.doi.org/10.1016/j.ymeth.2015.01.008

[39] Phadwal K, Alegre-Abarrategui J, Watson AS, Pike L, Anbalagan S, Hammond EM, Wade-Martins R, McMichael A, Klenerman P, Simon AK. A novel method for autophagy detection in primary cells: impaired levels of macroautophagy in immunosenescent T cells. Autophagy 2012; 8:677-89; PMID:22302009; http://dx.doi.org/10.4161/auto.18935

[40] Finn PF, Dice JF. Proteolytic and lipolytic responses to starvation. Nutrition 2006; 22:830-44; PMID:16815497; http://dx.doi.org/10.1016/j.nut.2006.04.008

[41] Cahill GF, Jr. Fuel metabolism in starvation. Annu Rev Nutr 2006; 26:1-22; PMID:16848698; http://dx.doi.org/10.1146/annurev.nutr.26.061505.111258

[42] Bouwens M, Afman LA, Muller M. Fasting induces changes in peripheral blood mononuclear cell gene expression profiles related to increases in fatty acid beta-oxidation: functional role of peroxisome proliferator activated receptor alpha in human peripheral blood mononuclear cells. Am J Clin Nutr 2007; 86:1515-23; PMID:17991667

[43] Hildebrandt W, Kinscherf R, Hauer K, Holm E, Droge W. Plasma cystine concentration and redox state in aging and physical exercise. Mech Ageing Dev 2002; 123:1269-81; PMID:12020948; http://dx.doi.org/10.1016/S0047-6374(02)00013-1

[44] Hine C, Harputlugil E, Zhang Y, Ruckenstuhl C, Lee BC, Brace L, Longchamp A, Treviño-Villarreal JH, Mejia P, Ozaki CK, et al. Endogenous hydrogen sulfide production is essential for dietary restriction benefits. Cell 2015; 160:132-44; PMID:25542313; http://dx.doi.org/10.1016/j.cell.2014.11.048

[45] Green DR, Galluzzi L, Kroemer G. Cell biology. Metabolic control of cell death. Science 2014; 345:1250256.

[46] Galluzzi L, Pietrocola F, Levine B, Kroemer G. Metabolic control of autophagy. Cell 2014; 159:1263-76; PMID:25480292; http://dx.doi.org/10.1016/j.cell.2014.11.006

[47] Lee C, Safdie FM, Raffaghello L, Wei M, Madia F, Parrella E, Hwang D, Cohen P, Bianchi G, Longo VD. Reduced levels of IGF-I mediate differential protection of normal and cancer cells in response to fasting and improve chemotherapeutic index. Cancer Res 2010; 70:1564-72; PMID:20145127; http://dx.doi.org/10.1158/0008-5472.CAN-09-3228

[48] Longo VD, Fontana L. Calorie restriction and cancer prevention: metabolic and molecular mechanisms. Trends Pharmacol Sci 2010; 31:89-98; PMID:20097433; http://dx.doi.org/10.1016/j.tips.2009.11.004

[49] Lee JV, Carrer A, Shah S, Snyder NW, Wei S, Venneti S, Worth AJ, Yuan ZF, Lim HW, Liu S, et al. Akt-dependent metabolic reprogramming regulates tumor cell histone acetylation. Cell Metab 2014; 20:306-19; PMID:24998913; http://dx.doi.org/10.1016/j.cmet.2014.06.004

[50] Comerford SA, Huang Z, Du X, Wang Y, Cai L, Witkiewicz AK, Walters H, Tantawy MN, Fu A, Manning HC, et al. Acetate dependence of tumors. Cell 2014; 159:1591-602; PMID:25525877; http://dx.doi.org/10.1016/j.cell.2014.11.020

[51] Mashimo T, Pichumani K, Vemireddy V, Hatanpaa KJ, Singh DK, Sirasanagandla S, Nannepaga S, Piccirillo SG, Kovacs Z, Foong C, et al. Acetate is a bioenergetic substrate for human glioblastoma and brain metastases. Cell 2014; 159:1603-14; PMID:25525878; http://dx.doi.org/10.1016/j.cell.2014.11.025

[52] Wang Z, Cao L, Kang R, Yang M, Liu L, Zhao Y, Yu Y, Xie M, Yin X, Livesey KM, et al. Autophagy regulates myeloid cell differentiation by p62/SQSTM1-mediated degradation of PML-RARalpha oncoprotein. Autophagy 2011; 7:401-11; PMID:21187718; http://dx.doi.org/10.4161/auto.7.4.14397

[53] Orfanelli T, Doulaveris G, Holcomb K, Jeong JM, Sisti G, Kanninen TT, Caputo TA, Gupta D, Witkin SS. Inhibition of autophagy in peripheral blood mononuclear cells by vaginal fluid from women with a malignant adnexal mass. Int J Cancer 2015; 137:2879-84; PMID:26132572; http://dx.doi.org/10.1002/ijc.29665

[54] Leveque-El Mouttie L, Vu T, Lineburg KE, Kuns RD, Bagger FO, Teal BE, Lor M, Boyle GM, Bruedigam C, Mintern JD, et al. Autophagy is required for stem cell mobilization by G-CSF. Blood 2015; 125:2933-6; PMID:25788702; http://dx.doi.org/10.1182/blood-2014-03-562660

[55] Remijsen Q, Vanden Berghe T, Wirawan E, Asselbergh B, Parthoens E, De Rycke R, Noppen S, Delforge M, Willems J, Vandenabeele P. Neutrophil extracellular trap cell death requires both autophagy and superoxide generation. Cell Res 2011; 21:290-304; PMID:21060338; http://dx.doi.org/10.1038/cr.2010.150

[56] Francois A, Julian A, Ragot S, Dugast E, Blanchard L, Brishoual S, Terro F, Chassaing D, Page G, Paccalin M. Inflammatory Stress on Autophagy in Peripheral Blood Mononuclear Cells from Patients with Alzheimer's Disease during 24 Months of Follow-Up. PLoS One 2015; 10:e0138326; PMID:26393801; http://dx.doi.org/10.1371/journal.pone.0138326